

Investigation on the thermal characteristic of MgO:PPSLT crystal by transmission spectrum of a swept cavity

JIAO WEI,¹ HUADONG LU,^{1,2,*} PIXIAN JIN,¹ AND KUNCHI PENG^{1,2}

¹State Key Laboratory of Quantum Optics and Quantum Optics Devices, Institute of Opto-Electronics, Shanxi University, Taiyuan, Shanxi 030006, China

²Collaborative Innovation Center of Extreme Optics, Shanxi University, Taiyuan, Shanxi 030006, China
*luhuadong@sxu.edu.cn

Abstract: A method of evaluating the thermal focal length of nonlinear crystal via transmission spectrum of a swept cavity (TSSC) is presented. By recording the resonant point offset of the TSSC, the thermal focal length can be successfully measured. Furtherly, by distinguishing the absorption of ultraviolet (UV) laser and UV laser induced infrared absorption (ULIIRA), it is clear that the ULIIRA is the important factor which induces the thermal lens effect compared to the absorption of UV laser for MgO-doped periodically poled stoichiometric lithium tantalate (MgO:PPSLT) crystal and it becomes serious with the increase of the generated UV laser. The ULIIRA coefficient measurement and thermal focal length evaluation of MgO:PPSLT crystal can supply an useful reference for researchers to generate high quality UV laser and squeezed or entangled state of optical field by using MgO:PPSLT crystal. The presented method can also be used to precisely evaluate the thermal focal length of other nonlinear crystals.

© 2017 Optical Society of America

OCIS codes: (140.3610) Lasers, ultraviolet; (140.3515) Lasers, frequency doubled; (140.6810) Thermal effects; (190.1450) Bistability; (140.3560) Lasers, ring.

References and links

1. R. T. White, I. T. Mckinnie, S. D. Butterworth, G. W. Baxter, D. M. Warrington, P. G. R. Smith, G. W. Ross, and D. C. Hanna, "Tunable single-frequency ultraviolet generation from a continuous-wave Ti:sapphire laser with an intracavity PPLN frequency doubler," *Appl. Phys. B* **77**, 547–550 (2003).
2. Z. Xu, Y. Wu, L. Tian, L. Chen, Z. Zhang, Z. Yan, S. Li, and H. Wang, "Long lifetime and high-fidelity quantum memory of photonic polarization qubit by lifting zeeman degeneracy," *Phys. Rev. Lett.* **111**, 240503 (2013).
3. V. Ruseva and J. Hald, "Generation of UV light by frequency doubling in BIBO," *Opt. Commun.* **236**, 219–223 (2004).
4. H. Lu, X. Sun, J. Wei, and J. Su, "Intracavity frequency-doubled and single-frequency Ti:sapphire laser with optimal length of the gain medium," *Appl. Opt.* **54**(13), 4262–4266 (2015).
5. W. Yang, Y. Wang, Y. Zheng, and H. Lu, "Comparative study of the frequency-doubling performance on ring and linear cavity at short wavelength region," *Opt. Express* **23**(15), 19624–19633 (2015).
6. A. A. Surin, T. E. Borisenko, and S. V. Larin, "Generation of 14 W at 589 nm by frequency doubling of high-power CW linearly polarized Raman fiber laser radiation in MgO:sPPLT crystal," *Opt. Lett.* **41**(11), 2644–2647 (2016).
7. M. Stappel, D. Kolbe, and J. Walz, "Continuous-wave, double-pass second-harmonic generation with 60% efficiency in a single MgO:PPSLT crystal," *Opt. Lett.* **39**(10), 2951–2954 (2014).
8. S. C. Kumar, G. K. Samanta, and M. Ebrahim-Zadeh, "High-power, single-frequency, continuous-wave second-harmonic-generation of ytterbium fiber laser in PPKTP and MgO:sPPLT," *Opt. Express* **17**(16), 13711–13726 (2008).
9. S. V. Tovstonog, S. Kurimura, and K. Kitamura, "High power continuous-wave green light generation by quasiphase matching in Mg stoichiometric lithium tantalate," *Appl. Phys. Lett.* **90**, 051115 (2007).
10. I. Ricciardi, M. D. Rosa, A. Rocco, P. Ferraro, A. Vannucci, P. Spano, and P. D. Natale, "Sum-frequency generation of cw ultraviolet radiation in periodically poled LiTaO₃," *Opt. Lett.* **34**(9), 1348–1350 (2009).
11. J. Hirohashi, K. Imai, H. Motegi, Y. Tomihari, T. Fukui, and Y. Furukawa, "Sub-watts 355 nm generation with 2nd- and 3rd- order-QPM PPMgSLT," in Conference on Lasers and Electro-Optics (OSA, 2010), p. CMG4.
12. H. Lu, J. Wei, Y. Wei, J. Su, and K. Peng, "Generation of high-power single-frequency 397.5 nm laser with long lifetime and perfect beam quality in an external enhancement-cavity with MgO-doped PPSLT," *Opt. Express* **24**(21), 23726–23734 (2016).
13. O. A. Louchev, N. E. Yu, S. Kurimura, and K. Kitamura, "Thermal inhibition of high-power second-harmonic generation in periodically poled LiNbO₃ and LiTaO₃ crystals," *Appl. Phys. Lett.* **87**, 131101 (2005).

14. Y. Yang, J. Wen, S. Wang, D. Cai, and Z. Guo, "The thermal lens focus of the end-pumped Nd:YAG laser," *Acta Photonica Sinica* **34**(12), 1769–1772 (2005).
15. A. Douillet, J.-J. Zondy, A. Yelisseyev, S. Lobanov, and L. Isaenko, "Stability and frequency tuning of thermally loaded continuous-wave AgGaS₂ optical parametric oscillators," *J. Opt. Soc. Am. B* **16**(9), 1481–1498 (1999).
16. R. Le Targat, J.-J. Zondy, and P. Lemonde, "75%-Efficiency blue generation from an intracavity PPKTP frequency doubler," *Opt. Commun.* **247**, 471–481 (2005).
17. X. Sun, J. Wei, W. Wang, and H. Lu, "Realization of a continuous frequency-tuning Ti:sapphire laser with an intracavity locked etalon," *Chin. Opt. Lett.* **13**(7), 071401 (2015).
18. Y. Sun, H. Lu, and J. Su, "Continuous-wave, single-frequency, all-solid-state Ti:Al₂O₃ laser," *Acta Sinica Quantum Optica* **14**(3), 344–347 (2008).
19. L. Holtmann, K. Buse, G. Kuper, A. Groll, H. Hesse, and E. Kratzig, "Photoconductivity and light-induced absorption in KNbO₄:Fe," *Appl. Phys. A* **53**, 81–86 (1991).
20. A. D. Ludlow, H. M. Nelson, and S. D. Bergeson, "Two-photon absorption in potassium niobate," *J. Opt. Soc. Am. B* **18**(12), 1813–1820 (2001).
21. Q. Yin, H. Lu, and K. Peng, "Investigation of the thermal lens effect of the TGG crystal in high-power frequency-doubled laser with single frequency operation," *Opt. Express* **23**(4), 4981–4990 (2015).
22. Q. Yin, H. Lu, J. Su, and K. Peng, "High power single-frequency and frequency-doubled laser with active compensation for the thermal lens effect of terbium gallium garnet crystal," *Opt. Lett.* **41**(9), 2033–2036 (2016).

1. Introduction

Single-frequency UV laser is a type of important laser source owing to its extensive applications in fields of bio-medicine, metrology, laser printing, high resolution spectroscopy and so on [1]. Especially, single-frequency UV laser can be used to pump an optical parametric oscillator (OPO) to generate squeezed or entangled state of optical field, whose wavelength can be resonant on the absorption line of alkali metal atoms [2]. So far, the main method of generating single-frequency UV laser is frequency doubling technology and there are various nonlinear crystals to act as the frequency doublers, such as lithium triborate (LBO), bismuth triborate (BIBO), periodically poled potassium titanyl phosphate (PPKTP) and so on. Though critical-phase-matching BIBO and LBO crystals have wide transparent range and are suitable to generate UV laser with high output power, intrinsic characteristics of walk-off effect make the beam of generated UV laser imperfect [3,4]. Compared to BIBO and LBO, quasi-phase-matched (QPM) PPKTP crystal receives the favor of majority of scientists owing to its advantage of being free of walk-off as well as high effective nonlinearity ($d_{\text{eff}}=10\text{pm/V}$) [5]. However, the second harmonic (SH) wavelength of 400 nm is close to the transmission window edge of KTP, the severe absorption of the generated UV laser and the intrinsic gray tracking limit the output power of the generated UV laser and shorten the lifetime of the crystal. Recently, a new nonlinear crystal MgO:PPSLT is attached to importance owing to its intrinsic advantages including high thermal conductivity, high photo-refractive damage as well as broad transmission wavelength range and has been successfully used to generate green and yellow lasers [6–9]. Some groups also used MgO:PPSLT crystals to generate UV laser, but the powers were all at low level [10, 11]. Recently, our group generated 407 mW continuous-wave (CW) single-frequency 397.5 nm UV laser with long lifetime and perfect beam quality by using a MgO:PPSLT crystal in an external enhancement cavity. The experimental results have revealed the superiority of the MgO:PPSLT crystal compared to other nonlinear crystals [12]. Furtherly, in this paper, we investigate the thermal characteristic of MgO:PPSLT crystal via the TSSC when it is used to generate 397.5 nm UV laser in an external enhancement cavity. The relationship between the thermal focal length and cavity detuning is firstly deduced. By recording the cavity detuning according to the observed TSSC, the source of thermal effect in the frequency doubling process is investigated. Compared the total cavity detuning to that caused by second harmonic wave (SHW) absorption, the ULIIRA is turned out to be existent in MgO:PPSLT crystal and the absorption coefficient is determined. Then the thermal focal length of MgO:PPSLT crystal at different intracavity power level is obtained experimentally.

2. Theoretical analysis

In order to obtain high power single-frequency 397.5 nm UV laser, a MgO:PPLT crystal was inserted into an external enhancement cavity which could increase the intensity by one or two orders of magnitude compared to the single-pass process. By optimizing the parameters of the external enhancement cavity, the maximal power of 407 mW was achieved. In that case, the TSSC was so wide that the laser could not stably be locked to the frequency of the injected fundamental wave (FW) laser, which was presented in our previous paper [12]. The observed TSSC could be attributed to the thermal effect of the MgO:PPLT crystal. It was expected that the heating of the MgO:PPLT crystal was due to the residual FW absorption and the SHW absorption as well as the ULIIRA. In order to furtherly quantify the role of thermal effect and research the thermal characteristic of the MgO:PPLT crystal, it is necessary to know the relationship between thermal focal length and the TSSC. Taking SHW absorption as well as ULIIRA into account and ignoring the FW absorption owing to its tininess [13], the thermal focal length of the MgO:PPLT crystal can be described as following [14],

$$\frac{1}{f} = \frac{1}{f_s} + \frac{1}{f_u} \quad (1)$$

where f is the total thermal focal length, f_s and f_u are the thermal focal length generated by SHW absorption and ULIIRA, respectively. According to the radial heat diffusion model [15], the thermal focal length of f_s and f_u can be expressed as,

$$f_s = \frac{\pi\omega^2}{2\eta P_s} \cdot \frac{K_C}{dn/dT} \quad (2)$$

and

$$f_u = \frac{\pi\omega^2}{\eta P_u} \cdot \frac{K_C}{dn/dT} \quad (3)$$

where ω is the waist radius of the FW laser in the center of nonlinear crystal, η is the thermal conversion coefficient, which equals to unit because the absorbed laser radiations are overall converted to heat, K_C and dn/dT are the thermal conductivity and thermo-optic coefficient of the nonlinear crystal, respectively. P_s , P_u are the absorbed power of SHW and ULIIRA, respectively, and can be expressed as [16],

$$P_s = [\exp(\frac{\alpha_s l}{2}) - 1] \Gamma_{eff} P^2 \quad (4)$$

and

$$P_u = [1 - \exp(-\alpha_u l)] P \quad (5)$$

where P is the total intracavity power of the FW, α_s , α_u are the absorption coefficient of SHW and ULIIRA, respectively. l and Γ_{eff} are the length and nonlinear conversion efficiency of the MgO:PPLT crystal, respectively. Owing to the distribution of the SHW laser in the nonlinear crystal is nonuniform, the waist radius of the SHW laser is defined as $\omega/\sqrt{2}$, which leads to the occurrence of the factor of 2 in the Eq. (2). At the same time, the thermal effect of MgO:PPLT crystal can result in the cavity detuning and the transmission scanning fringe of the cavity is broadened, which is given as [16]

$$\Theta = \frac{P_s F}{2\pi\lambda_\omega} \cdot \frac{dn/dT}{K_C} \quad (6)$$

and

$$\Delta = \frac{P_u F}{2\pi\lambda_\omega} \cdot \frac{dn/dT}{K_C} \quad (7)$$

where Θ and Δ are the cavity detuning caused by SHW absorption and ULIIRA, respectively. F and λ_ω are the finesse of the external enhancement cavity and wavelength of FW laser, respectively. Combining Eq. (1) to Eq. (7), the total thermal focal length f can be derived as following,

$$f = \frac{\omega^2 F}{2\lambda_\omega \cdot \Delta + 4\lambda_\omega \cdot \Theta} \quad (8)$$

It is clear that the thermal focal length of the MgO:PPLST crystal can be evaluated when the Θ and Δ are measured. In the experiment, Θ can be obtained by measuring the absorption rate of SHW, and the total cavity detuning $\Psi = \Theta + \Delta$ can be obtained by measuring the resonant point offset of the transmission spectrum, which is expressed as [15]

$$\Psi = \frac{\nu - \nu_0}{c/[L + l(n-1)]/2F} \quad (9)$$

where ν is the resonating frequency of doubling cavity at different pump power, ν_0 is the resonating frequency of cold cavity where the power of injected pump laser and generated UV laser are both so small that the heating of the MgO:PPLST crystal can be ignored, c is the speed of light in vacuum, n is the refractive index of the nonlinear crystal, L is the geometrical length of the cavity, $\nu - \nu_0$ is the resonant point offset of the transmission spectrum, and $c/[L + l(n-1)]/2F$ is the half-width at half-maximum (HWHM) of the cold cavity, which can be directly measured in experiment. Once the total cavity detuning Ψ and cavity detuning Θ caused by SHW absorption are measured, the ULIIRA coefficient α_u of the MgO:PPLST crystal and the total thermal focal length f can be further calculated.

3. Experimental setup

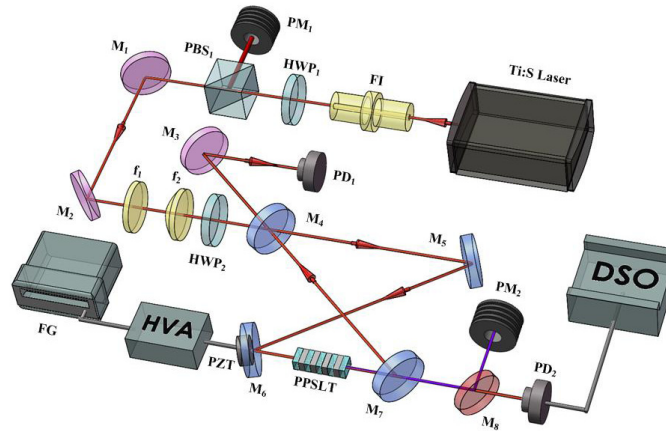


Fig. 1. Schematic of the experimental setup. HWP₁-HWP₂: half-wave plate; PBS₁: polarization beam splitter; PM₁-PM₂: power meter; PD₁-PD₂: photo detector; FG: function generator; HVA: high-voltage amplifier; DSO: digital storage oscilloscope.

In order to experimentally investigate the thermal characteristic of the MgO:PPLST crystal by TSSC, the experimental setup is sketched in Fig. 1. The FW laser is supplied by a homemade Ti:S laser which is pumped by a homemade single-frequency Nd:YVO₄ 532 nm laser with a maximal output power of 14 W [17, 18]. A Faraday isolator (FI) is adopted between the Ti:S laser and frequency doubling enhancement cavity to prevent the optical feedback into Ti:S laser. The power adjuster composed of a half-wave-plate (HWP₁) and a polarization beam splitter

(PBS₁) and HWP₂ before the enhancement cavity are used to adjust the incident pump power and ensure the polarization requirement for phase-matching condition of the MgO:PPLT crystal, respectively. The pump beam is coupled to the enhancement cavity by a telescopic system composed of two lenses f_1 ($f_1=110$ mm) and f_2 ($f_2=40$ mm). The enhancement cavity is formed by four mirrors, two flat mirrors (M₄ and M₅) and two plano-concave mirrors (M₆ and M₇) with 100 mm radius of curvature. M₄ is used as the input coupler and coated with the transmittance of 11% at 795 nm film. M₅ and M₆ are coated with high reflection (HR) film at 795 nm ($R_{795}>99.8\%$). M₇ is the output coupler and coated with HR film at 795 nm ($R_{795}>99.8\%$) and high transmittance (HT) film at 397.5 nm ($T_{397.5}>95\%$). The MgO:PPLT crystal with the dimension of $2\times 0.8\times 10$ mm³ is made by Oxide corporation and positioned at the center of M₆ and M₇. Two end faces of the crystal are coated with antireflection films for wavelength of both 795 nm and 397.5 nm. In order to precisely control the phase-matching temperature of the MgO:PPLT crystal, it is mounted in a small copper holder which is attached to a thermoelectric cooler (TEC). The reflected beam from M₄ is injected to a photo detector (PD₁) to lock the enhancement cavity to the frequency of the injected FW laser. The distance between M₆ and M₇ and total cavity length are 114.2 mm and 534 mm, respectively. In this case, the calculated radius of beam waist at the MgO:PPLT crystal is 42.18 μm which has been optimized, and the output power of the generated UV laser reaches up to 407 mW under the incident pump power of 1.9 W. The generated SHW laser are reflected by M₈ to a power meter (PM₂) to monitor the output power. The FW leaked from M₈ is detected by another photo detector (PD₂) and recorded by a digital storage oscilloscope (DSO) to record the TSSC.

4. Experimental results

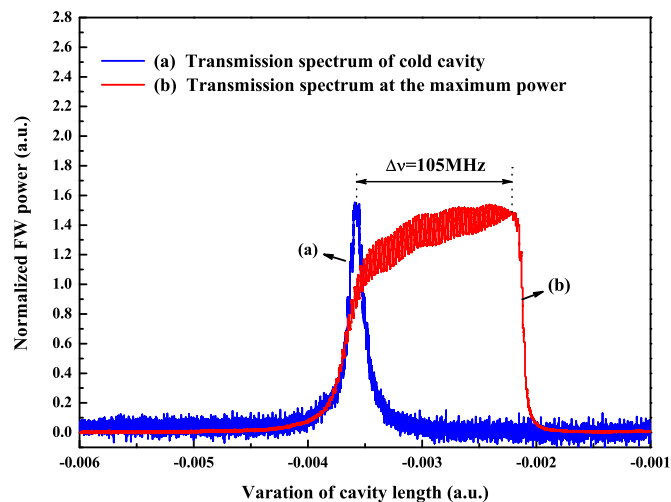


Fig. 2. The transmission spectra of frequency doubling cavity.

In the experiment, in order to obtain stable 397.5 nm UV laser, we had to lock the external enhancement cavity to the frequency of injected FW laser. To this end, a (30Hz 150V) triangle signal which was generated by a function generator (FG, DG1022U, RIGOL) and amplified by a homemade high-voltage amplifier (HVA, YG2009A, YG CO., Ltd), was used to scan the cavity to search for the resonant point. However, in this process, it was found that when the incident pump power gradually increased, the severe difference between the transmission spectrum of rising and falling edges was observed, which was attributed to the thermal effect of the

MgO:PPSLT crystal. The observed phenomenon, which was named bi-stability, was similar to that of the nonlinear crystals reported in other references [19–22]. In order to quantitatively evaluate the thermal focal length of the MgO:PPSLT crystal, we firstly recorded the resonant point offset of the transmission spectrum at the maximal incident pump power of 1.9 W, corresponding to the intracavity power of 35.33 W, relative to the cold cavity, which was shown in Fig. 2. It was clear that the measured scanning fringe was broadened $\nu - \nu_0 = 105$ MHz. With decrease of the incident pump power, the resonant point offsets were recorded in turn and the results were listed in Table.1. According to Eq. (9), the corresponding total cavity detuning of different intracavity power was obtained as shown in Fig. 3(a). The total cavity detuning increased with the increase of the intracavity power and reached up to $\Psi = 19$ when the intracavity power and the generated SHW power were 35.33 W and 414.5 mW, respectively.

Table 1. Frequency offset corresponding to different intracavity power

Cold cavity	FSR=550MHz	HWHM=5.51MHz	
Intracavity power/W	Offset/MHz	Intracavity power/W	Offset/MHz
35.33	105.05	24.27	46.13
34.36	97.08	23.58	33.64
33.16	88.88	21.60	18.39
30.62	85.05	19.93	12.26
28.76	74.63	18.45	6.13
27.37	70.72	16.71	3.83
25.49	60.07	14.01	2.29

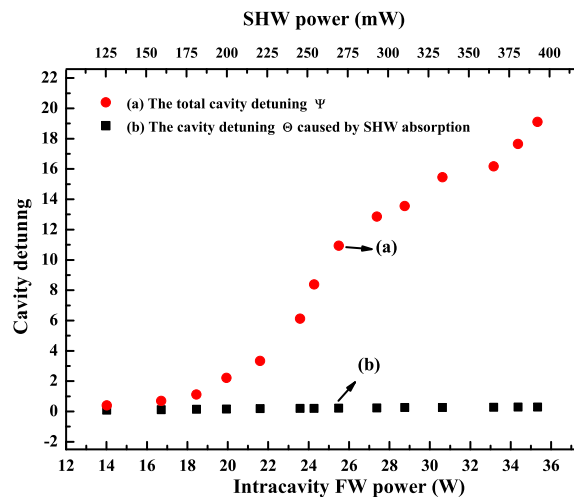


Fig. 3. The cavity detuning at different intracavity power level.

In order to further distinguish the contribution of the SHW absorption and ULIIRA to the total cavity detuning, the absorption of the 397.5 nm UV laser was solely measured by single-pass configuration with another 397.5 nm laser. The measured absorption efficiency at 397.5 nm was 4.5%, which was showed in Fig.4, and the corresponding absorption coefficient was $4.6\% \text{ cm}^{-1}$. On this basis, the cavity detuning Θ as a function of SHW power was plotted in Fig. 3(b). Comparing Figs. 3(a) to 3(b) demonstrated that the cavity detuning caused by SHW ab-

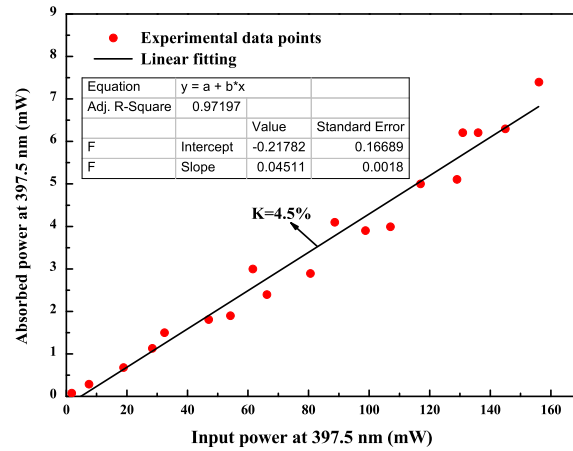


Fig. 4. Absorption at 397.5 nm of MgO:PPSLT.

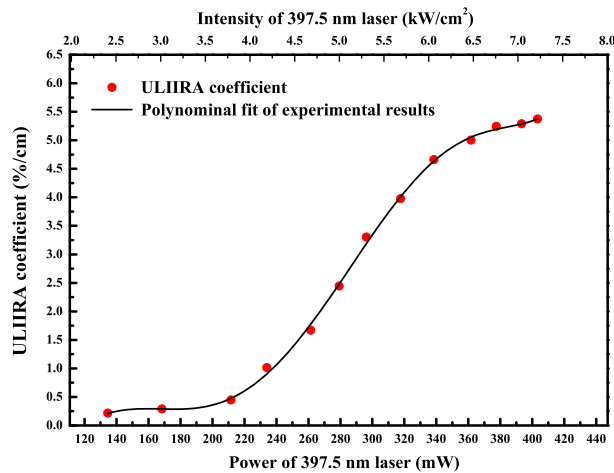


Fig. 5. ULIIRA coefficient as a function of internal UV laser.

sorption was much smaller than the total cavity detuning, which indicated that ULIIRA existed in MgO:PPSLT crystal and was really severe in high power region. Then the value of cavity detuning which was caused by ULIIRA was calculated. Therefore, the ULIIRA coefficient at different SHW power level were obtained and showed in Fig. 5. It indicated that the ULIIRA coefficient increased with the increasing of intensity of 397.5 nm laser internal to crystal. When the intensity was below 3.5 kW/cm^2 , the ULIIRA coefficient was as low as $0.5\% \text{ cm}^{-1}$. However, it increased rapidly when the intensity was larger than 4 kW/cm^2 . When the intensity was up to 7 kW/cm^2 , the ULIIRA coefficient was as large as $5.5\% \text{ cm}^{-1}$. As a result, the ULIIRA could lead to a severe thermal effect in high power region. After determining every part of cavity detuning, the total thermal focal length could be determined in turn by Eq. (8). The thermal focal length of MgO:PPSLT crystal as a function of intracavity power was plotted in Fig. 6. It showed that the thermal focal length was longer than 120 mm when the intracavity power was lower than 14 W. When the power increased from 14 W to 24 W, the thermal focal length was getting short rapidly. When the power increased continuously, the thermal focal length was up

to 3 mm, in this condition, the cavity was seriously influenced by the thermal effect, and could not operate steadily.

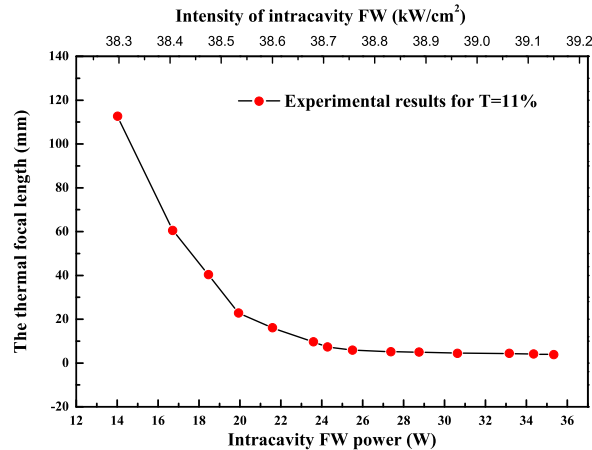


Fig. 6. The total thermal focal length at different circulating power level.

5. Summary

In summary, we have investigated the thermal characteristic of MgO:PPSLT crystal by the TSSC when it was used to generate the 397.5 nm UV laser. When the enhancement cavity was scanned with a triangle signal, the TSSC at different incident pump power were observed and recorded. Consequently, the total cavity detuning was measured and that caused by SHW absorption was also obtained with the measured absorption coefficient of $4.6\% \text{ cm}^{-1}$ of SHW. Comparing these two parts of cavity detuning, the ULIIRA was turned out to be existent in MgO:PPSLT crystal and the ULIIRA coefficient was investigated quantitatively. When the intensity of UV laser was below 3.5 kW/cm^2 , the ULIIRA coefficient was lower than $0.5\% \text{ cm}^{-1}$. With the increase of the UV laser intensity, it increased rapidly and reached up to $5.5\% \text{ cm}^{-1}$ when the UV laser intensity was up to 7 kW/cm^2 . At last, with the obtained two parts of cavity detuning, the total thermal focal length was obtained. When the intracavity FW power was higher than 24 W, the thermal focal length was lower than 3 mm. In addition, it showed that this severe thermal effect was mainly caused by ULIIRA. The ULIIRA coefficient measurement and thermal focal length evaluation of MgO:PPSLT crystal can supply an useful reference for researchers to generate high quality UV laser and squeezed or entangled state of optical field by using MgO:PPSLT crystal. The presented method can also be used to precisely evaluate the thermal focal length of other nonlinear crystals.

Funding

National Natural Science Foundation of China (NSFC) (Grant Nos. 61405107); Key Project of the Ministry of Science and Technology of China (Grant No. 2016YFA0301401); National Natural Science Foundation of China (Grant Nos. 61227015, 61227902, 61640404); National Fundamental Fund of Personnel Training (Grant No. J1103210).